

Charged Kaon Mass Measurement using the Cherenkov Effect

N. Graf^f A. Lebedev^d R. J. Abrams^{k,n} U. Akgun^j G. Aydin^j W. Baker^c P. D. Barnes, Jr.^g
 T. Bergfeld^ℓ L. Beverly^c A. Bujak^h D. Carey^c C. Dukes^m F. Duru^j G.J. Feldman^d A. Godley^ℓ
 E. Gülmez^{j,o} Y.O. Günaydin^j H. R. Gustafson^k L. Gutay^h E. Hartouni^g P. Hanlet^e S. Hansen^c
 M. Heffner^g C. Johnstone^c D. Kaplan^e O. Kamaev^e J. Kilmer^c J. Klay^g M. Kostin^c D. Lange^g J. Ling^ℓ
 M. J. Longo^k L. C. Lu^m C. Materniak^m M.D. Messier^f H. Meyer^{c,p} D. E. Miller^h S. R. Mishra^ℓ
 K. Nelson^m T. Nigmanov^k A. Norman^m Y. Onel^j J. M. Paley^f H. K. Park^k A. Penzo^j R. J. Petersonⁱ
 R. Raja^c D. Rajaram^k D. Ratnikov^e C. Rosenfeld^ℓ H. Rubin^e S. Seun^d N. Solomey^{e,p} R. Soltz^g
 E. Swallow^b R. Schmitt^c P. Subbarao^k Y. Torun^e T. E. Tope^c K. Wilson^ℓ D. Wright^g K. Wu^ℓ

^aBrookhaven National Laboratory, Upton NY 11973

^bElmhurst College, Elmhurst, IL 60126

^cFermi National Accelerator Laboratory, Batavia, IL 60510

^dHarvard University, Cambridge, MA 02138

^eIllinois Institute of Technology, Chicago, IL 60616

^fIndiana University, Bloomington, IN 47403

^gLawrence Livermore National Laboratory, Livermore, CA 94550

^hPurdue University, West Lafayette, IN 47907

ⁱUniversity of Colorado, Boulder, CO 80309

^jUniversity of Iowa, Iowa City, IA 52242

^kUniversity of Michigan, Ann Arbor, MI 48109

^ℓUniversity of South Carolina, Columbia, SC 29201

^mUniversity of Virginia, Charlottesville, VA 22904

ⁿCurrently at Muons, Inc., Batavia, IL 60510

^oAlso at Bogazici University, Istanbul, Turkey

^pCurrently at Wichita State University, Wichita, KS 67260

Abstract

The two most recent and precise measurements of the charged kaon mass use X-rays from kaonic atoms and report uncertainties of 14 ppm and 22 ppm yet differ from each other by 122 ppm. We describe the possibility of an independent mass measurement using the measurement of Cherenkov light from a narrow-band beam of kaons, pions, and protons. This technique was demonstrated using data taken opportunistically by the Main Injector Particle Production experiment at Fermi National Accelerator Laboratory which recorded beams of protons, kaons, and pions ranging in momentum from +37 GeV/c to +63 GeV/c. The measured value is 491.3 ± 1.7 MeV/c², which is within 1.4σ of the world average. An improvement of two orders of magnitude in precision would make this technique useful for resolving the ambiguity in the X-ray data and may be achievable in a dedicated experiment.

1. Introduction

The charged kaon mass is an important input in determining the CKM matrix element V_{us} from measurements of the branching ratio of $K^+ \rightarrow \pi^0 e^+ \nu$. The value of the charged kaon mass reported by the Particle Data Group is 493.677 MeV/c² with an uncertainty of 26 parts per million (ppm) [1]. This value is a weighted average of six measurements but is dominated by the two most recent and precise measurements from Denisov [2] and Gall [3] which measure

X-ray energies from kaonic atoms. While these measurements report uncertainties of 14 and 22 ppm they differ by 122 ppm (4.6σ). In this article we explore one possibility to resolve this discrepancy using an independent technique for measuring the charged kaon mass based on the Cherenkov effect. The well known pion and proton masses are used as references. The technique is demonstrated using data taken opportunistically using the Ring Imaging Cherenkov (RICH) sub-detector of the Main Injector Particle Production (MIPP) experiment at Fermilab [4].

2. Measurement Concept

Cherenkov light is emitted when a relativistic charged particle of mass m , momentum p , and speed $\beta = 1/\sqrt{1 + (m/p)^2}$ travels through a radiator volume of index of refraction n with $\beta > 1/n$. (As is customary in high energy physics we work in units in which the speed of light, c , is 1.) Neglecting dispersive effects for the moment, the light is emitted in a cone at an angle θ given by $\cos \theta = 1/\beta n$ [5,6] which is approximately

$$\theta = \sqrt{2\left(1 - \frac{1}{n\beta}\right)} \quad (1)$$

for small angles. Now, consider two particles i and j with identical momenta p but different masses m_i, m_j and speeds β_i, β_j . They will emit Cherenkov light at angles θ_i, θ_j which are related by the expression

$$\beta_i \theta_i^2 - \beta_j \theta_j^2 = 2(\beta_i - \beta_j). \quad (2)$$

In the relativistic limit $p \gg m$, $\beta \approx 1 - \frac{m^2}{2p^2}$. This, when combined with Eqn. 2, gives

$$\theta_i^2 - \theta_j^2 = \frac{m_j^2 - m_i^2}{p^2}, \quad (3)$$

where we have neglected the small difference between $\beta\theta$ and θ . If the particles i and j are pions, protons, and kaons, we have two independent angle-squared differences that can be measured

$$\theta_\pi^2 - \theta_K^2 = \frac{m_K^2 - m_\pi^2}{p^2}, \text{ and } \theta_\pi^2 - \theta_p^2 = \frac{m_p^2 - m_\pi^2}{p^2}. \quad (4)$$

Using these, the kaon mass is given by

$$m_K^2 = m_\pi^2 + \Delta_{p\pi} \frac{\theta_\pi^2 - \theta_K^2}{\theta_\pi^2 - \theta_p^2}, \quad (5)$$

where $\Delta_{p\pi} \equiv m_p^2 - m_\pi^2$. Notice that for a monochromatic beam in the absence of dispersion the index of refraction n and momenta p drop out. The kaon mass can be determined, in principle, through measurements of the pion and proton masses and the Cherenkov angles of the three particles. The proton and pion masses are known to 0.9 ppm and 2.5 ppm respectively and will not be the limiting factors in the experiment.

Using Eqn. 5 we can estimate the uncertainty in m_K^2 measured using this method as:

$$\sigma_{m_K^2}^2 = \sigma_{m_\pi^2}^2 + \left(\frac{\theta_\pi^2 - \theta_K^2}{\theta_\pi^2 - \theta_p^2}\right)^2 \sigma_{\Delta_{p\pi}}^2 + 4p^4 \left[\theta_\pi^2 \frac{\Delta_{pK}^2}{\Delta_{p\pi}^2} \sigma_{\theta_\pi}^2 + \theta_K^2 \sigma_{\theta_K}^2 + \theta_p^2 \frac{\Delta_{K\pi}^2}{\Delta_{p\pi}^2} \sigma_{\theta_p}^2 \right]. \quad (6)$$

The first two terms are due to the uncertainties in the pion and proton masses and are small. The third term grows with momentum and suggests that it is best to conduct the measurement at as low a momentum as possible where

the differences in the Cherenkov angles are largest, while staying above proton threshold.

In a RICH detector, the angle θ can be determined on a track-by-track basis from the pattern of Cherenkov photons recorded. However, the light for a single ring will be distributed about the central angle θ due to the variation of the index of refraction of the radiator medium over the wavelengths at which Cherenkov photons are produced. This gives as contribution to the uncertainty in the average angle θ determined from a single track of

$$\sigma_{\theta_i}^2 = \frac{1}{N_h} \left(\frac{1}{\theta_i n^2 \beta_i} \right)^2 \delta_n^2, \quad (7)$$

where δ_n is the size of the variation in the index of refraction over wavelengths relevant to the detection mechanism and N_h is the number of photomultiplier tube (PMT) hits in the ring.

In a beamline, particles will be accepted if their momentum lies in a narrow window about some central value p . The finite size of this momentum acceptance window introduces an additional uncertainty in the average angle measured from a single track. Averaging over N_r rings, the momentum spread contributes an uncertainty

$$\sigma_\theta^2 = \frac{1}{N_r} \left[\sigma_{\theta_i}^2 + \left(\frac{m_i^2 \beta_i}{\theta_i n p^2} \right)^2 (\sigma_p/p)^2 \right] \quad (8)$$

to the measurement of θ , where σ_p is the spread in the beam particle momenta about their central value. Taking the specific case of an experiment using CO₂ as the radiator ($n = 1.00045$, $\delta_n = 7 \times 10^{-6}$) and a beam of central momentum 40 GeV/c with a width of $\sigma_p/p=0.01$, the statistical uncertainty in the kaon mass is

$$\frac{\sigma_{m_K}^2}{m_K^2} = 0.6^2 + 0.9^2 + \frac{7.3^2}{N_\pi} + \frac{14.2^2}{N_K} + \frac{10.1^2}{N_p} [\text{ppm}]^2, \quad (9)$$

where the first term results from uncertainties in the pion mass, the second from uncertainties in the proton mass, and the final three terms result from uncertainties in the angles θ_π , θ_K , and θ_p with N_π , N_K , and N_p being the number of millions of pion, kaon, and proton rings recorded. Using Eqn. 9 we find that the uncertainty is minimized if 32% of the data is collected using protons, 23% using pions, and 45% using kaons. This result is only weakly dependent on momentum as shown in Fig. 1 which plots the expected statistical precision of the charged kaon mass as a function of momentum choice and total number of rings recorded. With 10 million rings at 40 GeV/c, we expect a statistical precision of 10 ppm using this technique.

3. RICH detector overview

The RICH detector used by MIPP was built by the SELEX Collaboration [7] for use in that experiment. We summarize here only the most important features of the detector as deployed for the MIPP experiment and refer the reader to [8,9,10,11] for details.

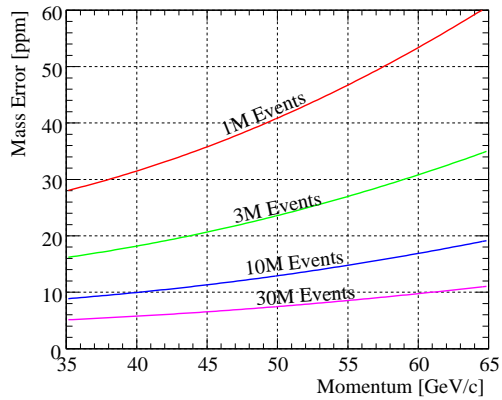


Fig. 1. Expected statistical uncertainty for kaon mass measurement.

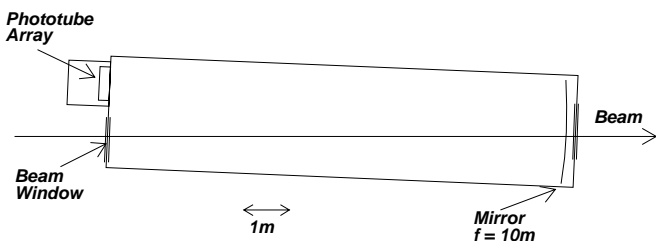


Fig. 2. Schematic of the RICH detector [8].

The geometry of the RICH counter is shown in Figure 2. The detector was constructed from a low carbon cylindrical steel vessel 10.22 m in length and 93 in. in diameter with a wall thickness of $\frac{1}{2}$ in. The ends were sealed with 1.5 in. thick aluminum flanges that were cut out to hold thin beam windows at each end and a photomultiplier tube holder plate at the upstream end. The vessel was wrapped by a water line carrying chilled water and 15 cm of building insulation to regulate the temperature.

A $2.4\text{ m} \times 1.2\text{ m}$ array of 16 mirrors mounted at the downstream end of the counter focused Cherenkov light on an array of $\frac{1}{2}$ in. photomultiplier tubes. On average the mirrors had a radius of curvature of 1980 cm with variations less than 5 cm and a reflectivity of more than 85% at 160 nm.

MIPP used CO_2 gas held at just above atmospheric pressure as the radiator. At STP, CO_2 has an index of refraction of 1.00045 at $\lambda = 300$ nm giving thresholds of $p = 4.5$ GeV/c for pions, 17 GeV/c for kaons, and 31 GeV/c for protons. The gas temperature and pressure were continuously monitored enabling calibration of the index of refraction. A $\beta = 1$ particle produced a ring of radius 29.5 cm and an average of 30 PMT hits providing 3σ π/K separation up to 80 GeV/c and 3σ p/K separation up to 120 GeV/c. Figure 3 shows sample event displays for each beam species showing PMT hits and reconstructed rings.

The PMTs were mounted in a hexagonal array behind a 2 mm thick quartz window which provided a gas-tight seal between the phototubes and the radiator volume. They were read out in threshold (on/off) mode. Two models of PMTs were used: Hamamatsu R760 and Russian made FEU60. The FEU60 tubes were coated with a wavelength

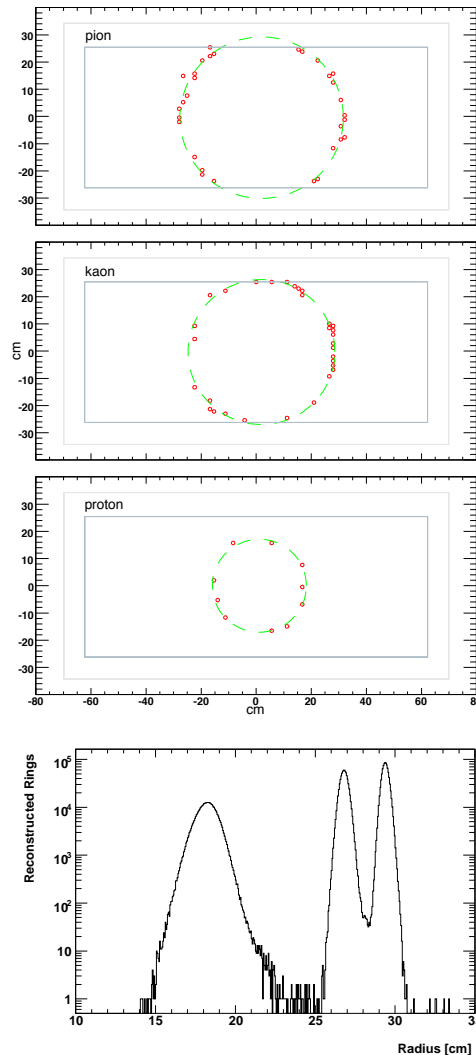


Fig. 3. Sample event displays of 40 GeV pion (top), kaon (middle), and proton (bottom) rings in the RICH counter. Small circles indicate hit PMTs. The large dashed circles show the rings reconstructed from the PMT hits. The final plot is the distribution of reconstructed ring radii for 40 GeV.

shifter to match the acceptance region of the R760's. The R760 (FEU60) tubes have a maximum quantum efficiency of about 25% (11%) at 350 nm. Of the available 89 PMT columns, 68 were used, with R760's installed in 15 columns and FEU60's installed in 53 columns. The front-end electronics of the RICH detector was re-designed and rebuilt by the MIPP collaboration.

4. Data Analysis

In outlining the measurement concept, we made several simplifying assumptions which must be accounted for during analysis. Due to dispersion, Cherenkov light is not observed at a single angle, but as a distribution across several angles. In our analysis, we measured the average PMT occupancies for pion, proton, and kaon rings as a function of Cherenkov angle in data and compared them to calculations

which incorporated the kaon mass as a free parameter. In total 12 million rings were recorded for this measurement using positively charged beams of pions, kaons, and protons ranging from 37 GeV/c to 63 GeV/c in momentum.

In the data, wire chambers upstream and downstream of the RICH counter were used to reconstruct the particle trajectory and predict the center of the RICH ring. Using that prediction for the center position, a Cherenkov angle was assigned to each PMT and the average probability for a PMT to fire was computed as a function of Cherenkov angle, as shown in Fig. 5. This procedure was done separately for each PMT type, mirror, and momentum setting. As the measurement was made with beam particles, light struck only the two central mirrors, labeled 8 and 9.

To compare to the data, we calculated the expected occupancy of each PMT in the RICH array for pion, proton, and kaon rings. The calculation starts with the number of Cherenkov photons produced per unit path length between wavelengths λ and $\lambda + d\lambda$ [5,6]:

$$\frac{d^2 N_{ph}}{d\lambda dx} = \frac{2\pi\alpha}{\lambda^2} \sin^2 \theta_C, \quad (10)$$

where α is the fine structure constant. These photons travel through the radiator medium, reflect off mirrors, pass through a quartz window, and are collected by a reflective cone before they are incident on the photodetector. The transmission probability for a Cherenkov photon of wavelength λ for each of these steps is plotted in Fig. 4 along with the photodetector efficiency. Combining these factors, the average number of photoelectrons detected by PMT i is given by

$$N_{pe}^i = \int_0^L \int_{\theta_1}^{\theta_2} \int_{\lambda_1}^{\lambda_2} \frac{2\pi\alpha}{\lambda^2} \left(1 - \frac{1}{n^2(\lambda)\beta^2}\right) e^{-\mu(\lambda)(F_L+x)} \otimes S(\theta, \theta_C(\lambda)) \epsilon(\lambda) G_i(\theta) d\lambda d\theta dx \quad (11)$$

where $\epsilon(\lambda)$ is the product of all wavelength-dependent efficiency factors, $\mu(\lambda)$ is the absorption coefficient of CO₂, F_L is the mirror focal length, and G_i is the geometric acceptance of the i^{th} PMT. Scattering of light from angular bin θ_C to bin θ is accounted for by the function $S(\theta, \theta_C)$. The light scattering was modeled as a Gaussian of width σ with three components. These include an intrinsic term independent of wavelength and a wavelength-dependent dispersive term [12]. A third term accounts for multiple scattering of the beam particle in the RICH radiator:

$$\sigma^2 = \sigma_0^2 + \frac{\sigma_N^2}{\tan^2 \theta_C} + \sigma_{ms}^2 \quad (12)$$

where σ_0 is the intrinsic scattering width and σ_n is the dispersive scattering width. The calculated shapes are implicitly functions of the particle masses through β . Using Poisson statistics, the probability for a PMT seeing N_{pe} photoelectrons to be on is:

$$P = 1 - \exp(-N_{pe} - b), \quad (13)$$

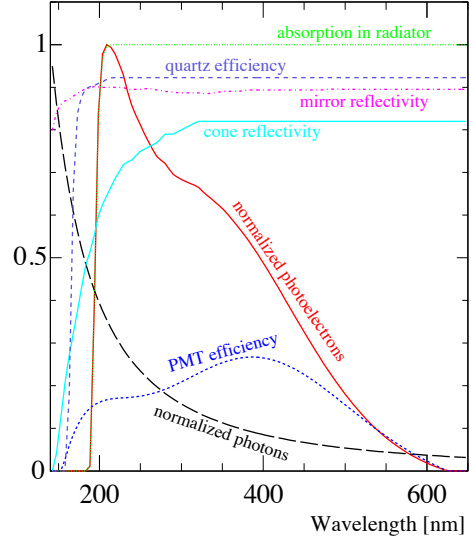


Fig. 4. Overlay of all efficiency functions incorporated into the calculation of detector photoelectrons as a function of angle. Also shown are the initial Cherenkov photon production spectrum and final photoelectron yield normalized to peak at 1 for inclusion in the plot.

where b accounts for the PMT dark noise rate.

The measured and calculated PMT occupancies were compared using a χ^2 statistic. In the comparison several parameters were allowed to vary to minimize χ^2 . These were:

- i. Intrinsic detector smearing width, σ_0
- ii. Dispersive smearing width, σ_N
- iii. Density ratio scaling factor
- iv. Density ratio offset
- v. Level of air contamination in CO₂
- vi. Central pion momentum
- vii. Width of momentum distribution
- viii. Kaon mass

The density ratio is defined as the gas density inside the RICH divided by density at STP and was varied to account for uncertainties in the calibration of the pressure and temperature monitors installed in the counter.

The momentum acceptance of the beamline was modeled as a Gaussian and uncertainties in the mean and width of this acceptance were incorporated into the calculation. The average proton and kaon momenta accepted by the beamline differ slightly from the average pion momentum due to variations in particle production at the secondary target. This effect was incorporated using a simulation of the copper secondary target using the FLUKA [13,14] production model.

After all known effects were accounted for there were $\mathcal{O}(10\%)$ differences between the measured and calculated PMT occupancies, due presumably to our incomplete understanding of the factors which control Cherenkov photon production and transport in our detector. To account for these differences, the uncertainties in the PMT occupancies were increased until $\chi^2/ndf = 1$ was achieved at the minimum. The scaling factor ranged from about 25 to 100

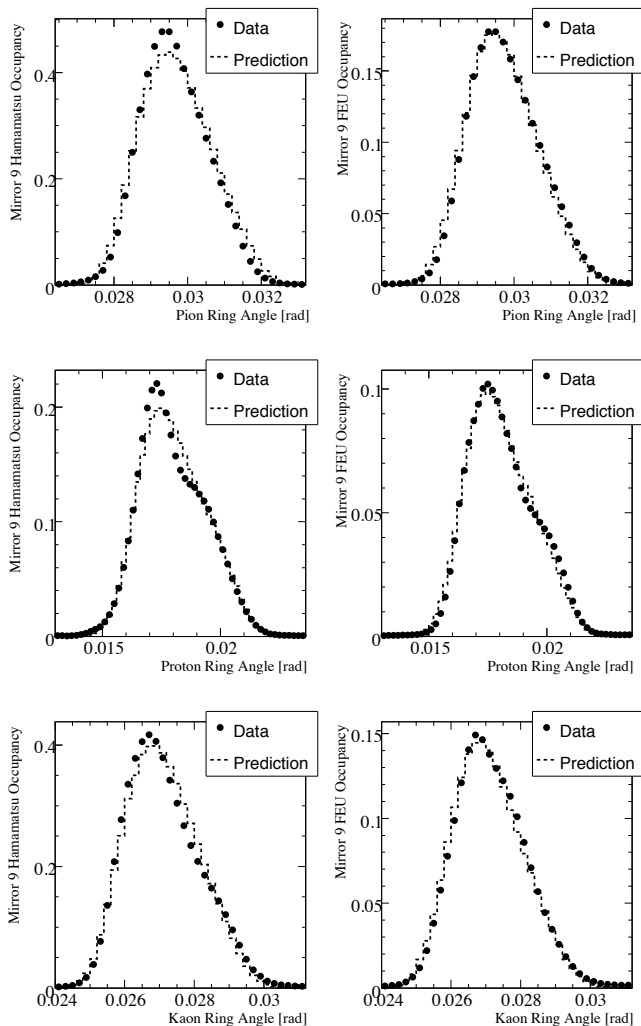


Fig. 5. Comparison of measured PMT occupancies to best-fit predictions for 40 GeV data set [15]. Pions are shown in the top row, protons in the middle row, and kaons in the bottom row. In each row, the left panel shows the results for R760 PMTs while the right panel shows the results for FEU60 PMTs.

for the different combinations of PMT type, mirror, and beam momentum. Systematic uncertainties overwhelm the statistical uncertainties for this data set. A sample fit for 40 GeV/ c data is shown in Figure 5.

Kaon mass results for each data set are shown in Fig. 6. Using just the low momentum data sets results in a kaon mass measurement of 491.9 ± 1.1 MeV; using just the high momentum data sets gives 486.7 ± 3.0 MeV. These results agree within uncertainties and are combined to give a final result for the charged kaon mass of 491.3 ± 1.7 MeV (3500 ppm). The convention of scaling error bars when combining measurements so that $\chi^2/n_{df} = 1$ is followed resulting in a larger final uncertainty. This result is within 1.4σ of the PDG value [1].

See [15] for a detailed discussion of the analysis presented in this paper.

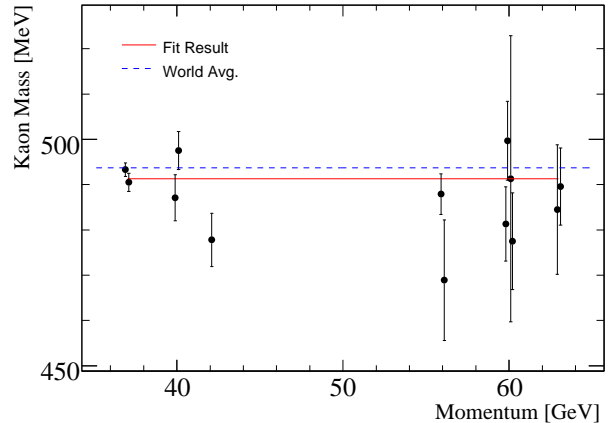


Fig. 6. Summary of kaon mass results for data sets using various beam momenta and mirrors. At each momentum setting, results for mirror 8 are plotted shifted slightly to the left, while results for mirror 9 are plotted shifted slightly to the right. The solid line shows the final kaon mass result, and the dotted line is the accepted value from the PDG.

5. Suggestions for Improvement

The largest systematic uncertainty in this measurement is the dependence of PMT occupancy on Cherenkov angle. This is a result of the effect on the geometric acceptance of the PMT array by the selection of reliable PMT hits and the detailed understanding of the detector response as a function of wavelength. The geometric acceptance calculation was complicated by cross-talk in the readout electronics – a problem which manifested itself during the high rate conditions the detector was operated under for this measurement. Occasionally, a single PMT hit would cause all 16 channels sharing the same readout board to register a hit. This effect was difficult to model and introduced considerable uncertainty in the geometric acceptance of the PMT array. Finally, in our analysis we characterized each PMT using an average PMT response. A measurement of the PMT response on a tube-by-tube basis would have required dis-assembly of the detector, which we did not undertake. Knowledge of the photodetector response on a channel-by-channel basis would reduce uncertainties in the occupancy calculation.

Assuming that the geometric and spectral response of the photodetectors is well known, other sources of systematic uncertainty would need to be controlled more precisely. A better understanding of the optical properties of the radiator would be necessary to compete with the precision of the X-ray measurements. Maintaining consistent performance with a gaseous detector, where both the pressure and temperature must be carefully controlled, may be unworkable. An aerogel maintained at a uniform temperature would have a stable refractive index and a higher light yield per unit of path length. It would also be helpful to have a single focusing mirror, so that Cherenkov light would not be divided among different mirrors with different focal lengths.

Uncertainties due to the π , K , and p beam momenta could be controlled by narrowing the momentum acceptance of the beamline. If further reductions in uncertainties are required, track-by-track reconstruction of the particle momentum could be implemented.

In our detector, we used 1/2" diameter phototubes with digital (on/off) readout. Photodetectors (for example hybrid photodetectors) are available which could provide finer sampling of the ring shapes and reliable photoelectron counts as a function of angle.

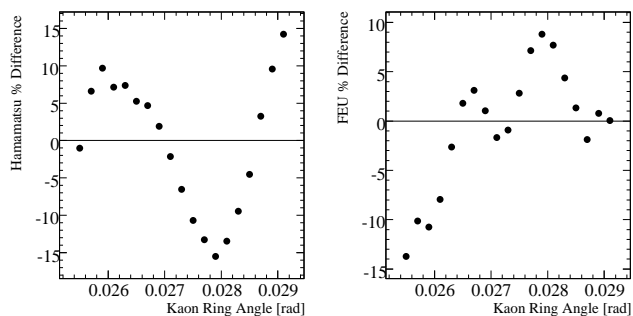


Fig. 7. Percent difference between data and predicted occupancy for 40 GeV/c kaons. Hamamatsu tubes are on the left, FEU tubes are on the right.

In conclusion, an improvement of two orders of magnitude in the precision would make this technique competitive for resolving the 122 ppm discrepancy in the X-ray measurements. As shown in Fig. 7, our comparison of the PMT occupancies to our expectations agree within 5-15% near the peaks of the occupancy distributions. If this uncertainty could be reduced to 1% it should be possible to realize the statistical potential of this technique. We believe this could be achieved in a dedicated experiment with careful study and control of the systematics discussed in this section.

Acknowledgments Fermilab is operated by Fermi Research Alliance, LLC under Contract No. DE-AC02-07CH11359 with the United States Department of Energy.

References

- [1] C. Amsler, et al., Particle data group, Phys. Lett. B667 1 (2008) 704.
- [2] A. Denisov, et al., New measurement of the mass of the K^- meson, JEPT Lett. 54 (1991) 558.
- [3] K. Gall, et al., Precision measurement of the K^- and σ^- masses, Phys. Rev. Lett. 60 (1988) 186.
- [4] MIPP Collaboration, <http://ppd.fnal.gov/experiments/e907/>.
- [5] V. Zrelov, Cherenkov Radiation in High-Energy Physics, Israel Program for Scientific Translations, Ltd., 1970.

- [6] J. Jelley, Cherenkov Radiation and its Applications, Pergamon Press, 1958.
- [7] SELEX Collaboration, <http://fn781a.fnal.gov>.
- [8] J. Engelfried, et al., The SELEX phototube RICH detector, Nucl. Instr. and Meth. A 431 (1999) 53–69.
- [9] J. Engelfried, et al., The RICH detector of the SELEX experiment, Nucl. Instr. and Meth. A 433 (1999) 149–152.
- [10] J. Engelfried, et al., The e781 (SELEX) RICH detector, Nucl. Instr. and Meth. A 409 (1998) 439–442.
- [11] L. Stutte, J. Engelfried, J. Kilmer, A method to evaluate mirrors for Cherenkov counters, Nucl. Instr. and Meth. A 369 (1996) 69.
- [12] R. Forty, O. Scheider, *RICH pattern recognition*, LHCb technical note number LHCb/98 040, <http://lhcb.web.cern.ch/lhcb-rich/html/lhcb-rich.notes.htm> (1998).
- [13] A. Fasso', A. Ferrari, J. Ranft, P. Sala, FLUKA: a multi-particle transport code, CERN 2005-10, INFN/TC.05/11, SLAC-R-773 (2005).
- [14] A. Fasso', et al., The physics models of FLUKA: status and recent developments, in: Computing in High Energy and Nuclear Physics Conference, 2003.
- [15] N. J. Graf, Measurement of the charged kaon mass with the MIPP RICH, Ph.D. thesis, Indiana University, Bloomington, IN (August 2008).